Evaluation of Bogus Vortex Techniques with Four-Dimensional Variational Data Assimilation

Zhao-Xia Pu

Goddard Earth Sciences and Technology Center, University of Maryland Baltimore County, Catonsville, Maryland, and Laboratory for Atmospheres, NASA Goddard Space Flight Center, Greenbelt, Maryland

Scott A. Braun

Laboratory for Atmospheres, NASA Goddard Space Flight Center, Greenbelt, Maryland

ABSTRACT

The effectiveness of a four-dimensional variational data assimilation (4DVAR) technique for creating "bogus" vortices in numerical simulations of hurricanes is evaluated in this study. A series of numerical experiments is conducted to generate initial vortices for Hurricane Georges and Bonnie (1998) in the Atlantic Ocean by assimilating bogus sea level pressure and wind information into a mesoscale numerical model (MM5). Several different strategies are tested for investigating the sensitivity of the initial vortex representation to the type of bogus information.

While some of the results in this study confirm conclusions made in previous studies, some significant differences are obtained regarding the role of bogus wind data in creating a realistic bogus vortex. In contrast with previous studies in which the bogus wind data had only a marginal impact on creating a realistic hurricane, this study concludes that the wind information is *very important* because 1) with assimilation of only bogus sea level pressure information, the response in wind field is contained largely within the divergent component, with strong low-level convergence leading to strong upward motion near the center; and 2) with assimilation of bogus wind data only, an expected dominance of the rotational component of the wind field is generated. In this latter case, the minimum pressure is also adjusted significantly, although the adjusted sea level pressure does not always match the actual hurricane minimum pressure. The generated vortex offers a smooth start to the forecast and leads to a significant improvement in the forecast. Only when both the bogus sea level pressure and wind information are assimilated together does the model produce a vortex that represents the actual intensity of the hurricane and results in significant improvements to forecasts of both hurricane intensity and track.

As the 4DVAR experiments are performed with relatively coarse horizontal grid resolution in this study, the impact of vortex size on the structure of the initial vortex is also evaluated. The authors find that when the scale of the specified bogus vortex is smaller than that which can be resolved by the model, the assimilation method may result in structures that do not completely resemble observed structures in hurricanes. In contrast, when the vortex is sufficiently large for it to be resolved on the horizontal grid, but not so large as to be unrealistic, more reasonable hurricane structures are obtained.

1. Introduction

Forecasts of track and intensity changes for mature hurricanes require accurate representation of the hurricane vortex in model initial conditions. Vortices contained in large-scale analyses from operational centers are often too weak and sometimes misplaced and observations in the vicinity of the hurricane are usually sparse. In order to improve the storm representation, the use of so-called bogus vortices is often adopted (Lord 1991; Kurihara et al. 1990; Leslie and Holland 1995). A bogus vortex is an artificial vortex specified according to the size of the cyclone (the radius of maximum winds), its position, and its intensity (the maximum velocity or minimum sea level pressure). Traditionally, such bogus vortices have been directly implanted into the larger-scale environment. Many successful simulations, including prediction of hurricane movement and structure, have been conducted using bogus vortices for hurricane model initialization (e.g., Kurihara et al. 1990; Lord 1991; Trinh and Krishnamuti 1992). However, an important issue in such an approach is the consistency of the vortex with the properties of the prediction model (Iwasaki et al. 1987; Mathur 1991).

A more advanced scheme has been proposed by Kurihara et al. (1993) at the Geophysical Fluid Dynamics Laboratory (GFDL) to overcome such defects. The main strategy of their scheme is to replace the poorly resolved

Corresponding author address: Dr. Zhao-Xia Pu, NASA/GSFC, Code 912, Greenbelt, MD 20771.
E-mail: pu@agnes.gsfc.nasa.gov

vortex from a coarse-resolution analysis with a more realistic vortex that is constructed to better match the high-resolution hurricane prediction model. They apply two spatial filters to remove the poorly resolved vortex from the large-scale analysis. The specified vortex to be placed in the environmental field consists of a symmetric vortex and an asymmetric flow. The symmetric component is generated from a time integration of an axisymmetric version of the hurricane prediction model, with an observationally derived constraint imposed on the tangential flow. The generated symmetric wind is used in the computation of the asymmetric component using a simplified barotropic vorticity equation, thus providing consistent symmetric and asymmetric components. The mass field is then recomputed using a static initialization method in which the generated wind field is not modified. This technique, proposed by Kurihara et al. (1993), ensures the following desirable conditions: 1) a smooth transition between the environmental and storm fields; 2) compatibility of the specified vortex to the resolution and physics of the prediction model; 3) structural consistency of the generated vortex in the fields of wind, temperature, surface pressure, and moisture; and 4) the incorporation of realistic features in the tangential flow of the vortex. As anticipated, the method shows a substantial improvement in the track prediction (Bender et al. 1993). The success of this technique indicates the importance of having a dynamically and thermodynamically consistent initial vortex that is compatible with the resolution and physics of the hurricane prediction model.

As a natural extension of the GFDL's initialization method, Zou and Xiao (2000) have proposed a new approach to improve the initial vortex by using a four-dimensional variational data assimilation technique (4DVAR). The method requires two steps: 1) Specification of a bogus vortex by defining the position, radius of maximum surface wind (RMW), and minimum sea level pressure (SLP) of the initial vortex, and prescribing a symmetric SLP distribution over the vortex region; and 2) assuming that the time tendency of SLP is small in a short time period and then assimilating the specified bogus SLP field into the numerical model within a 30-min assimilation window. They show very encouraging results for Hurricane Felix (1995).

The advantages of using the 4DVAR technique to generate the bogus vortex are as follows. First, the 4DVAR technique uses the actual forecast model rather than a simplified model (e.g., an axisymmetric model) to provide a strong dynamical constraint during the bogus data assimilation. Observational data, bogus information, and model dynamics are combined in one system. The assimilation results not only fit the data but also are consistent with the model resolution and physics. Second, the 4DVAR technique allows all model variables to be adjusted freely during the assimilation period. Finally, the 30-min assimilation window allows the initially symmetric vortex to develop some asymmetric structures.

In a recent study, Xiao et al. (2000) applied the 4DVAR bogusing technique to Hurricane Fran (1996) and examined the impact of the specified vortex size and the relative impacts of bogus SLP and wind data. The initial vortex size affected both the track and intensity of the assimilated hurricane, with larger vortices generally moving somewhat to the left of smaller vortices and having weaker intensity. Their results also suggested that while the best results were obtained by assimilating both SLP and wind data, assimilation of the SLP only was much more effective in reproducing the 3D hurricane structure than assimilation of wind data only. Assimilation of winds only failed to reproduce the warm temperature anomaly and low surface pressure in the eye. According to their results, Xiao et al. (2000) concluded that the wind information had relatively small impact.

However, in many cases, such as that of hurricanes over the Pacific Ocean, reliable pressure information may not generally be available. In addition, satellite remotely sensed winds are frequently available over the ocean and may be of benefit for hurricane initialization. In order to explore further the effectiveness of the bogusing technique, this study reexamines the impact of wind information by applying the bogusing technique of Zou and Xiao (2000) to Hurricanes Georges and Bonnie over the Atlantic Ocean in 1998. Brief descriptions of the methodology and model are described in section 2. Evaluation of model sensitivity to the bogus vortex schemes and vortex size for Hurricane Georges (1998) is given in section 3. Results for Hurricane Bonnie (1998) are summarized in section 4. Discussion of the differences between this study and Zou and Xiao (2000) and Xiao et al. (2000) are given in section 5. Conclusions are provided in section 6.

2. A variational bogus vortex scheme

Similar to Zou and Xiao (2000) and Xiao et al. (2000), the bogus data assimilation technique consists of two steps: 1) Bogus vortex data specification and 2) 4DVAR assimilation of the bogus data.

a. Vortex specification

The bogus "observations" for the specified initial vortex consist of values of SLP and wind speed and direction over a circular region with a radius R. The vortex is assumed to be axisymmetric. The SLP field is specified based upon the RMW in the cyclone, the position of the hurricane center, and central pressure. In general, the distribution of bogus SLP data can be generated by empirical functions. In this study, the hurricane SLP is specified following the analytic model proposed by Holland (1980).

According to Holland (1980), the SLP, p^{bogus}, at radius r ($0 \leq r \leq R$) is defined by the following relationship:

$$p^{\text{bogus}}(r) = p_c + (p_n - p_c) \exp(-A/r^B), \qquad (1)$$

where p_c is the central pressure and p_n is the ambient pressure (theoretically at infinite radius; however, here it is taken from representative values in the hurricane environment). The scaling parameters A and B are defined by maximum wind information as follows. Using the gradient balance relationship and Eq. (1), the wind profile is

$$V_g^{\text{bogus}}(r) = \left[\frac{AB(p_n - p_c) \exp(-A/r^B)}{\rho r^B} + \frac{r^2 f^2}{4} \right]^{1/2} - \frac{rf}{2}, \qquad (2)$$

where V_g^{bogus} is the gradient surface wind at radius r, f is the Coriolis parameter, and ρ the air density (assumed constant at 1.15 g m^{-3}). In the region of maximum winds, the Coriolis force is small in comparison to the pressure gradient and centrifugal forces and the air is in cyclostrophic balance. These winds are given by

$$V_g^{\text{bogus}}(r) = [AB(p_n - p_c) \exp(-A/r^B)/(\rho r^B)]^{1/2}. \qquad (3)$$

By setting $dV_g/dr = 0$, the RMW is $R_m = A^{1/B}$ and substitution back into (3) gives the maximum wind speed, $V_m = C(p_n - p_c)^{1/2}$, where $C = (B/\rho e)^{1/2}$ and e is the base of the natural logarithm. Specification of V_m and R_m then provides values of A and B for Eqs. (1)–(2).

A vertical profile is assumed for the wind information in order to extend the information to higher levels. Following Kurihara et al. (1993), the vertical structure of the wind is specified by an empirical function $F(\sigma)$ as follows:

$$V_g^{\text{bogus}}(r, \sigma) = F(\sigma) V_g^{\text{bogus}}(r), \qquad (4)$$

where σ denotes the model vertical level. The numerical values of $F(\sigma)$ can be modified according to the storm depth (e.g., Kurihara et al. 1993).

b. Variational assimilation of the bogus vortex data

The bogus distributions of pressure and wind are introduced into the 4DVAR assimilation system within a 30-min assimilation window. The cost function to be minimized is written as follows:

$$J = \sum_{k=1,m} J_k + J_b, \qquad (5)$$

where J_b is the background term and J_k is the contribution to the cost function from a certain type of data. The subscript k denotes the type of data and m is the total number of available data types. For example, the contributions from bogus SLP and wind information can be described as

$$J_1 = \sum_{t_\tau} \sum_{i,j \in R} (\mathbf{p} - \mathbf{p}^{\text{bogus}})^{\text{T}} \mathbf{W}_p (\mathbf{p} - \mathbf{p}^{\text{bogus}}), \qquad (6)$$

$$J_2 = \sum_{t_\kappa} \sum_{(i,j,\sigma) \in R} (\mathbf{V} - \mathbf{V}_g^{\text{bogus}})^{\text{T}} \mathbf{W}_V (\mathbf{V} - \mathbf{V}_g^{\text{bogus}}), \qquad (7)$$

where $\mathbf{p}$ and $\mathbf{V}$ are the analysis variables; $\mathbf{p}^{\text{bogus}}$ and $\mathbf{V}^{\text{bogus}}$ are the bogus vortex data; (i, j) is the model horizontal grid location within R; t_τ and $t_\kappa \in (0, \Delta)$ are the observational times for SLP and wind, respectively; while Δ is the length of assimilation window. Further, $\mathbf{W}_p$ and $\mathbf{W}_v$ are weighting factors that depend on the assumed statistical error characteristics of the bogus data.

In this study, J_b is a simple background term measuring the distance between the model state and the mesoscale model analysis based on the large-scale European Centre for Medium-Range Weather Forecasts (ECMWF) analysis. Only approximated variances are included in the background weighting matrix.

c. The numerical forecast model and its adjoint

The Pennsylvania State University–National Center for Atmospheric Research (PSU–NCAR) mesoscale forecast model version 5 (MM5) and its adjoint system are used in this study. The MM5 is a limited-area, nonhydrostatic primitive equation model with multiple options for various physical parameterization schemes (Dudhia 1993; Grell et al. 1995). The model employs a terrain-following σ vertical coordinate, where σ is defined as $\sigma = (p - p_{\text{top}})/(p_{\text{sfc}} - p_{\text{top}})$, p is pressure, and p_{sfc} and p_{top} are the pressures at the surface and model top, respectively. Physics options used for the forecast model in this study include the Betts–Miller cumulus parameterization, a simple ice microphysics scheme (Dudhia 1993), the Blackadar high-resolution planetary boundary layer parameterization scheme (Blackadar 1976, 1979; Zhang and Anthes 1982), and a cloud atmospheric radiation scheme (Dudhia 1993). The land surface temperature is predicted using surface energy budget equations as described in Grell et al. (1995). For a more detailed description of MM5, the reader is referred to Dudhia (1993) and Grell et al. (1995).

The MM5 adjoint modeling system (Zou et al. 1998) is employed in the data assimilation experiment. For the variational data assimilation system, physics options are limited to the Kuo cumulus parameterization and a simple bulk aerodynamic planetary boundary layer scheme. Application of the MM5 adjoint model to a variety of mesoscale weather systems has been demonstrated in papers by Kuo et al. (1996) and Zou and Xiao (2000).

3. Evaluation of the variational bogus vortex scheme with Hurricane Georges (1998)

a. Summary of Hurricane Georges (1998)

Georges was the second deadliest and second strongest hurricane within the Atlantic basin during the 1998 season. During its 17-day lifetime (15 September–1 October), it
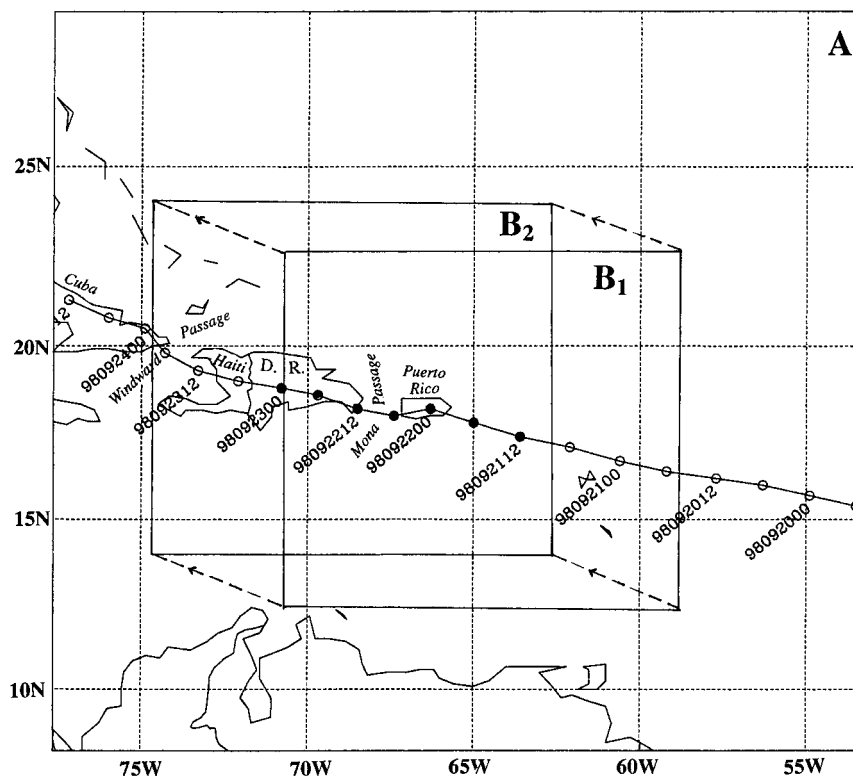
FIG. 1. Location of the model domains for Hurricane Georges (1998). Domain A is the 36-km grid and domain B is the nested, 12-km grid used in the forecast. Domain B is moved during the simulation from B1 to B2 at 15 h. Estimates of the center location at 6-h intervals from the Hurricane Research Division of NOAA are marked by circles. The period included in the simulation is marked by the bold segment of the track.

resulted in multiple landfalls, extending from the north-eastern Caribbean to the coast of Mississippi, and 602 fatalities, mainly in the Dominican Republic and Haiti.

Because of an interest in examining the landfall of Georges in Puerto Rico and Hispaniola, 1200 UTC 21 September 1998 was selected as the initial time for simulation. At this time, Georges was located over the ocean to the east-southeast of Puerto Rico (Fig. 1) and was a mature category 2 hurricane based on the Saffir–Simpson intensity scale, having recently weakened from category 4 intensity. Georges's eyewall made landfall in Puerto Rico with sustained surface winds in excess of 50 m s^{-1} late on 21 September. The hurricane moved inland over Puerto Rico, weakened slightly, and then moved into the Mona Passage early on 22 September, where it reintensified slightly before making landfall later that morning in the Dominican Republic with estimated sustained surface winds of 54 m s^{-1}. During the next 21 h, George weakened as it moved slowly across the mountainous terrain of the Dominican Republic and Haiti, where it produced copious rain, deadly flash floods, and mud slides. The system moved into the Windward Passage on the morning of 23 September with maximum sustained winds reduced to 33 m s^{-1}. Georges

changed little before making landfall in eastern Cuba later that afternoon (Fig. 1).

b. Experimental design

For the experiments, two horizontal grids are used, a fixed outer domain A, with 76 × 70 grid points and a 36-km grid spacing, and a nested, movable inner mesh B with 106 × 97 grid points and a 12-km grid spacing (Fig. 1). The model vertical structure is composed of 27 σ levels with the top of the model set at a pressure of 50 hPa. The σ levels are placed at values of 1.0, 0.99, 0.98, 0.96, 0.93, 0.89, then decreasing to 0 at an interval of 0.04. Considering the large computational expense and computer memory requirements of the 4DVAR technique, the assimilation of the bogus vortex information is applied only to the 36-km domain. At the end of the assimilation window (30 min), the 12-km nest is initialized by interpolation (see Grell et al. 1995) of all prognostic variables from the 36-km mesh using a monotonic interpolation scheme based upon Smolarkiewicz and Grell (1992). All figures present results from the 12-km grid.

Initial conditions for the 36-km domain, prior to as-

a)

MAXIMUM VECTOR: 27.2 m s⁻¹ →

b)

MAXIMUM VECTOR: 44.9 m s⁻¹ →

c)

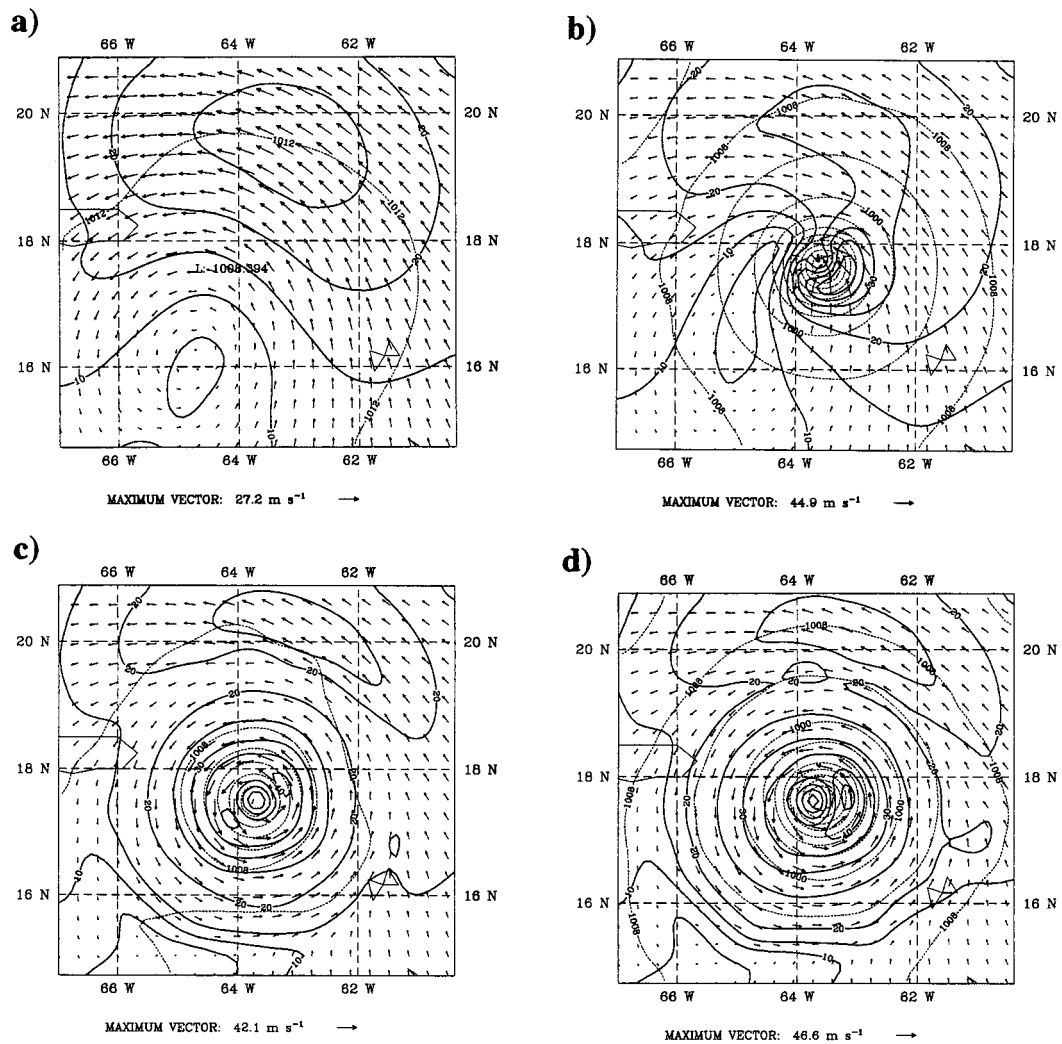MAXIMUM VECTOR: 42.1 m s⁻¹ →

d)

MAXIMUM VECTOR: 46.6 m s⁻¹ →

FIG. 2. Distributions of the SLP (thin dashed line, 4-mb interval), horizontal wind vectors, and wind speed (thick solid line, 5 m s⁻¹ interval) at 850 hPa at the end of the assimilation window (30 min). (a) CTRL analysis without the bogus vortex (Ctrl. 1), (b) assimilation of SLP only (Expt. 1), (c) assimilation of wind data only (Expt. 2), and (d) assimilation of both pressure and wind data (Expt. 3).

simulation, are derived from 12-h ECMWF analyses archived at NCAR. Analysis fields, including temperature, relative humidity, geopotential height, and winds at mandatory pressure levels and with horizontal resolution of 2.5° × 2.5°, are interpolated horizontally to model grid points and then refined by adding information from standard twice daily rawinsondes and 3-hourly surface and buoy reports using a Barnes objective analysis technique (Manning and Haagenson 1992). Final analyses are then interpolated to the model σ levels. The MM5 initial conditions derived from the ECMWF analysis are designated as the control analysis or "CTRL analysis." Figure 2a shows the CTRL analysis fields of SLP and 850-hPa wind vectors and wind speed at 1200 UTC 21 September 1998 for a portion of the 12-km domain centered on the storm. At the time, Hurricane George was a category 2 hurricane, but the CTRL anal-

ysis shows only a weak pressure minimum (about 1008 hPa) and a broad wind speed maximum to the northeast of the center.

Several experiments (see Table 1) are conducted using the four-dimensional variational assimilation of bogus data. The distribution of SLP in each case is specified following Holland's (1980) hurricane pressure profile [Eq. (1)] assuming, based upon observations, a central pressure of $p_c = 966$ hPa; a center location at 17.4°N, 63.6°W; an ambient pressure of $p_n = 1010$ hPa; a maximum surface wind speed of $\mathbf{V}_m = 48.9$ m s⁻¹; and an RMW of $R_m = 40$ km (estimated from airborne radar data). The bogus information extends out to a radius of 300 km. A control simulation (Ctrl. 1) is performed in which no bogus vortex is included in the initial conditions. Three experiments are conducted that vary the information assimilated into the model.
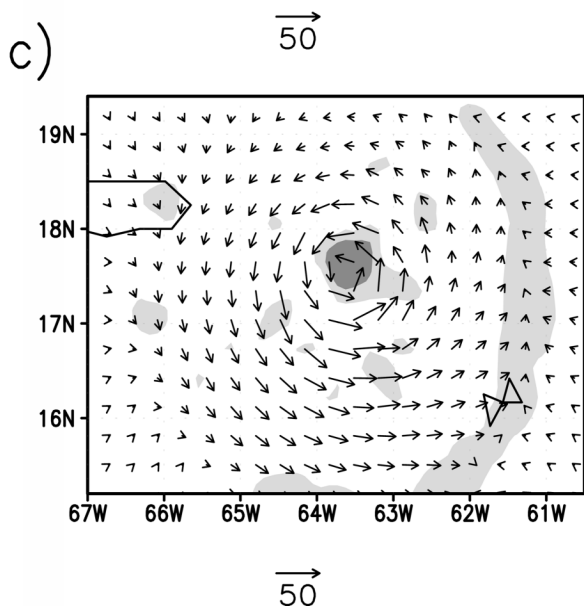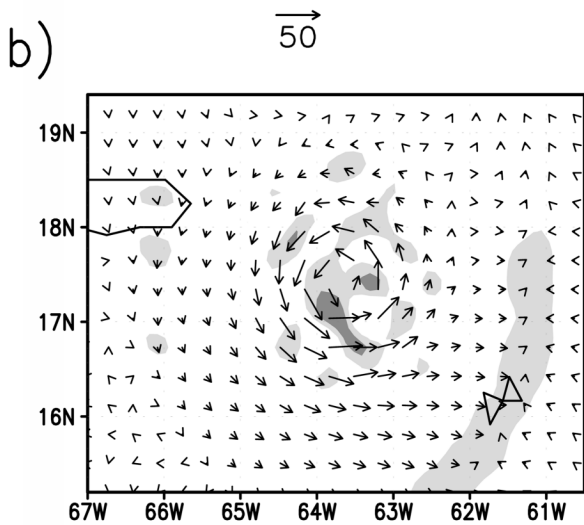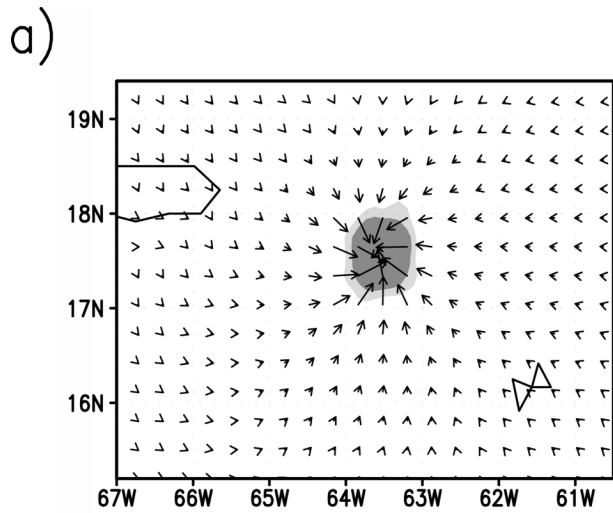
a)

TABLE 1. Experimental design.

Numerical experiments	Hurricane case	Bogus data assimilated	RMW (km)	Model initial condition
Ctrl. 1	Georges			CTRL analysis
Expt. 1	Georges	P^{bogus}	40	4DVAR analysis
Expt. 2	Georges	V_g^{bogus}	40	4DVAR analysis
Expt. 3	Georges	P^{bogus}, V_g^{bogus}	40	4DVAR analysis
Expt. 4	Georges	P^{bogus}	120	4DVAR analysis
Expt. 5	Georges	P^{bogus}, V_g^{bogus}	120	4DVAR analysis
Ctrl. 2	Bonnie			CTRL analysis
Expt. 6	Bonnie	P^{bogus}	120	4DVAR analysis
Expt. 7	Bonnie	V_g^{bogus}	120	4DVAR analysis
Expt. 8	Bonnie	P^{bogus}, V_g^{bogus}	120	4DVAR analysis

- Expt. 1: Similar to Zou and Xiao (2000), only bogus SLP data are assimilated into the mesoscale model, that is, $J = J_1 + J_b$.
- Expt. 2: Only bogus wind data are assimilated into the mesoscale model, that is, $J = J_2 + J_b$.
- Expt. 3: Both wind and SLP data are assimilated into the model, that is, $J = J_1 + J_2 + J_b$.

In Expts. 2 and 3, the surface wind is specified by the relationship in (2) and extended into the vertical following Kurihara et al. (1993) using (4) with the following vertical profile: $F(\sigma) = 1.0, 0.95, 0.85, 0.65, 0.35, 0.15$ for $\sigma = 0.9, 0.75, 0.5, 0.4, 0.3, 0.15$, respectively, and 0 above $\sigma = 0.15$. Sensitivity tests with different profile for $F(\sigma)$ indicate little sensitivity to reasonable variations of $F(\sigma)$. The weightings in Eq. (6) and (7) are treated as constants. We take $W_p = 1$ hPa^{-2} and $W_v = 0.1$ m^{-2} s^2 for all experiments (corresponding to 1-hPa pressure error and about 3 m s^{-1} wind error).

The specified SLP information is assimilated every 5 min within a 30-min window. The wind information is assimilated every 10 min in this 30-min window. This method assumes that the tendencies of SLP and wind are near zero during this half-hour. Zou and Xiao (2000) indicated that such constraints could be incorporated by adding a penalty term to the cost function.

b)

c)

c. Sensitivity of initial vortex to the type of bogus data

1) INITIAL VORTEX

For the assimilation experiments, minimization of the cost function generally converges in about 20–30 iter-

←

FIG. 3. Vector wind differences between Expts. 1–3 and control simulation at 850 hPa, for (a) Expt. 1, (b) Expt. 2, and (c) Expt. 3. The shading indicates horizontal divergence, with light shading indicating values less than -10^{-4} s^{-1} and dark shading indicating values less than -6×10^{-4} s^{-1}.
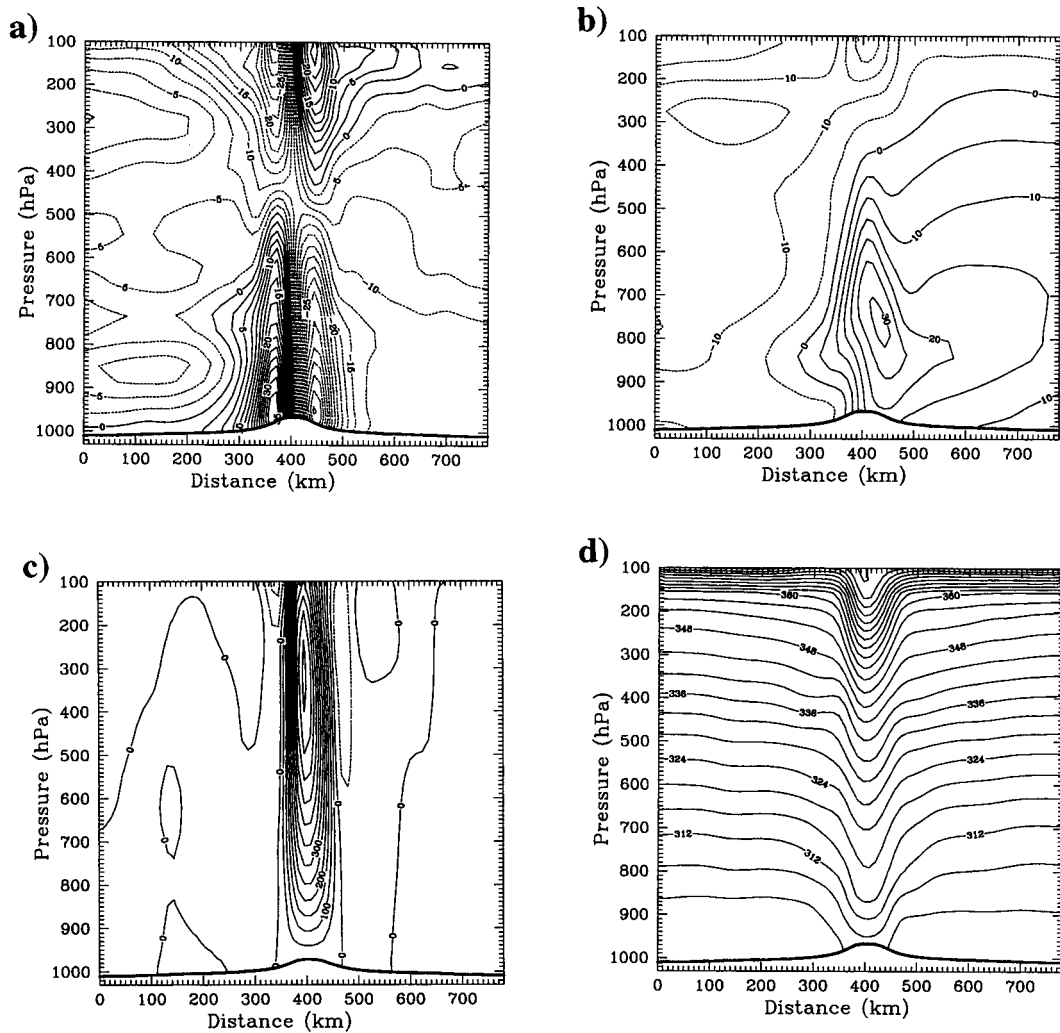
FIG. 4. East–west cross sections through the center of the vortex (17.4°N, 63.6°W) at the end of the assimilation window (30 min) for Expt. 1. (a) Zonal wind (u, 2.5 m s^{-1} contour interval), (b) meridional wind (v, 5 m s^{-1} interval), (c) vertical velocity (50 cm s^{-1} interval), and (d) potential temperature (θ, 4 K interval).

ations. In order to compare the experiments equally, the minimization is stopped after 30 iterations for all experiments. During the minimization procedure, the assimilation variables (SLP and/or winds) are forced toward the bogus information, while all other variables (e.g., temperature and moisture) are free to develop in a model-consistent manner. The improvement in the structure of the initial vortex is apparent after the assimilation procedure. Figure 2 shows the distribution of the initial SLP, wind speed, and wind vectors at 850 hPa before (Fig. 2a) and after data assimilation (Figs. 2b–d). The vortices after variational data assimilation are more intense than the vortex in the CTRL analysis. The winds show a more realistic distribution and maximum winds occur closer to the vortex center. Although a symmetric wind and/or SLP is assimilated during the minimization procedure, the resulting wind speed dis-

tribution includes an asymmetric structure in all three assimilation experiments.

The impacts of the assimilation of SLP and wind information, both separately and combined, are clearly seen in the horizontal flow. Figure 3 shows the initial vector wind differences between the experiments (Expts. 1, 2, and 3) and the control simulation as well as the divergence field at 850 hPa. When only bogus SLP information is assimilated (Expt. 1), the model response in the wind field is contained largely in the divergent component of the wind, with strong convergence leading to strong upward motion in the center (Fig. 4c). In contrast, assimilation of only the bogus winds (which are nondivergent) leads to an expected dominance of the rotational component of the wind field and a weakly convergent flow near the eye. *Only when both the bogus surface pressure and wind information*
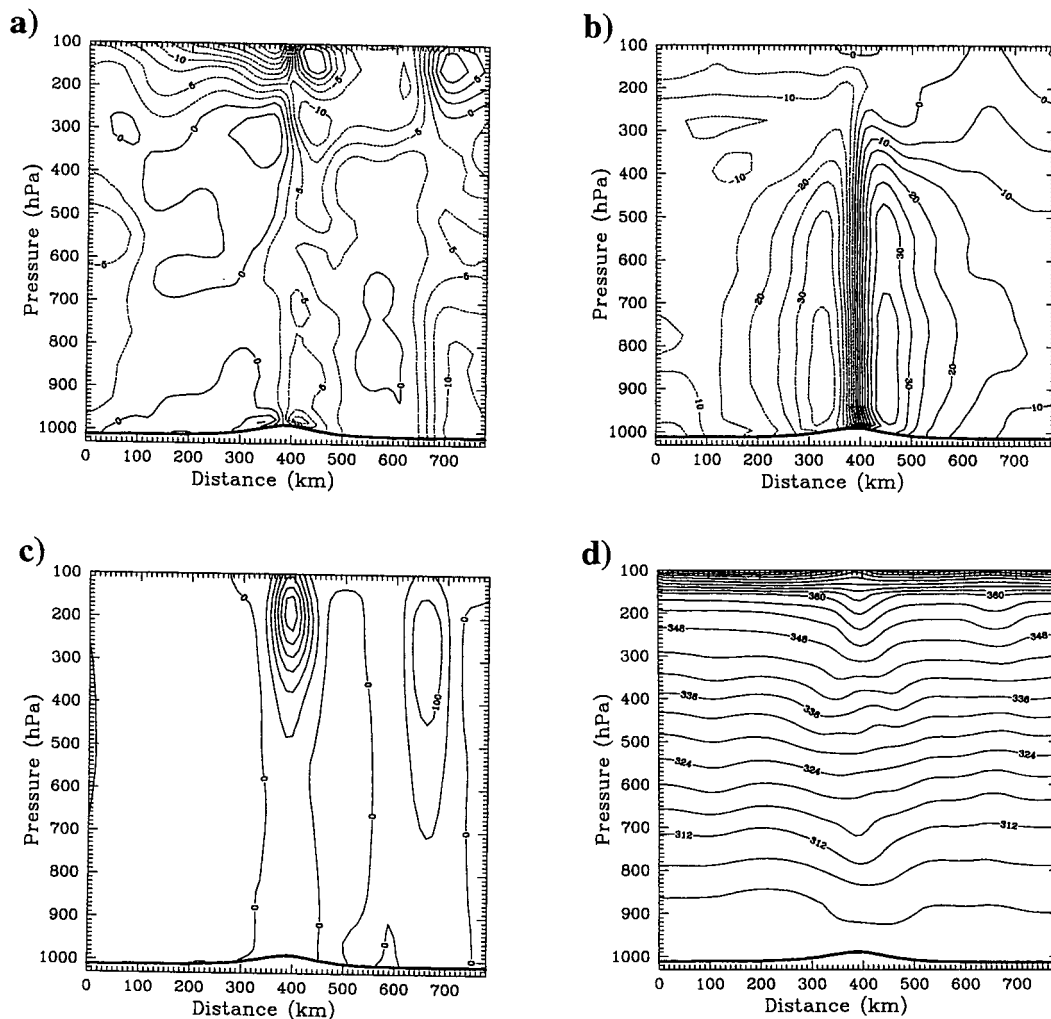
a)

b)

c)

d)

FIG. 5. Same as Fig. 4, except for Expt. 2.

are assimilated together does the model produce strong rotational and convergent wind fields (Fig. 3c). These results show that it is necessary to introduce the bogus wind information into the vortex initialization in order to get a more realistic structure of the vortex. In fact, the effects of including bogus wind information derived from the gradient balance equation is equivalent to introducing a gradient balance constraint during data assimilation. The model forces the vortex wind field to be consistent with the gradient balance relationship, but it also allows the system to reproduce both rotational and convergent components of the wind field during the short assimilation window.

The vertical structures of the bogus vortices vary considerably between the experiments. Figure 4 shows vertical cross sections through the center of the storm of the zonal, meridional, and vertical velocities, as well as potential temperature for Expt. 1, in which only bogus SLP information was assimilated. Consistent with the strong convergence seen at the surface (Fig. 3a), the

zonal velocity (Fig. 4a) depicts strong convergence below and strong divergence above 500 hPa, which leads to strong upward motion (Fig. 4c) and a large warm potential temperature anomaly (Fig. 4d) in the center of the storm. The meridional velocity field (Fig. 4b) shows a strong southerly jet on the eastern side of the storm, but only very weak northerly flow on the western side; in other words, assimilation of only SLP information fails to produce a reasonable vortex in this case. In Expt. 2, in which only bogus wind information was assimilated, the model response is dominated by the rotational component (Fig. 3b), and the model produces a fairly symmetric vortex in the meridional wind field (Fig. 5b). The zonal component shows much weaker perturbations near the center, implying much weaker low-level convergence and upper-level divergence. Consequently, much weaker vertical motions (Fig. 5c) occur in the center in Expt. 2 compared to Expt. 1, with the maximum upward motion occurring in the upper troposphere. A weak potential temperature anomaly is produced in
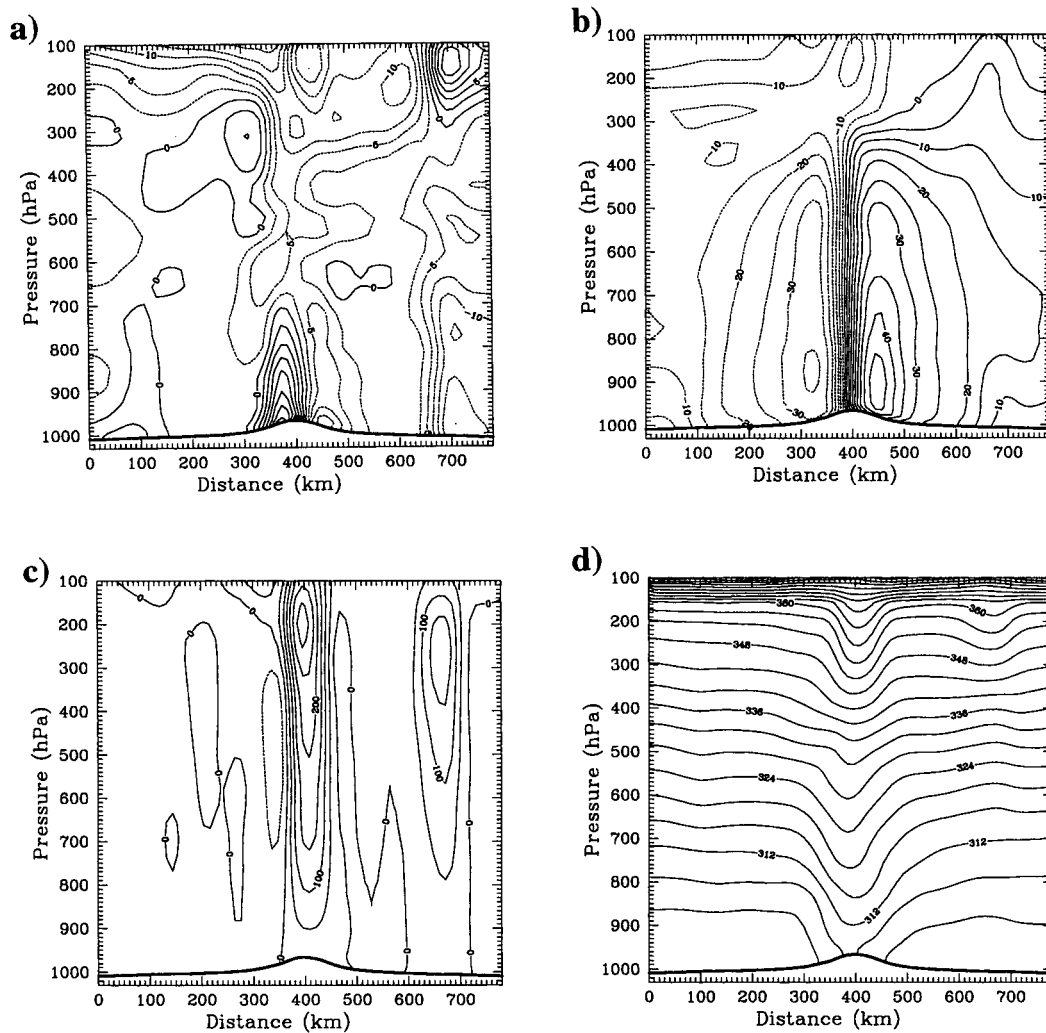
FIG. 6. Same as Fig. 4, except for Expt. 3.

Expt. 2, a result that differs from Xiao et al. (2000), who found no warm anomaly whatsoever in their wind-only assimilation case (see Fig. 15a of Xiao et al. 2000). Figure 6 shows cross sections for Expt. 3 in which both SLP and wind information are assimilated. The meridional velocities (Fig. 6b) show a well-developed asymmetric vortex with winds greater than 45 m s^{-1} on the eastern side and only 30–35 m s^{-1} on the western side. The radial velocities (Fig. 6a) imply stronger (weaker) low-level inflow and convergence than that seen in Expt. 2 (Expt. 1). Upward motions (Fig. 6c) are comparable to Expt. 2 but extend through the depth of the troposphere. The warm potential temperature anomaly in the center is comparable to Expt. 1 at lower to middle levels, but it is much weaker in the upper troposphere. This result is consistent with the findings of Xiao et al. (2000).

In each experiment, the strongest upward motions occur near the center of the storm, unlike observed vertical motions in hurricanes, in which the upward motion is displaced from the center in the form of an eyewall. This simulated structure results from the fact that the 36-km horizontal grid spacing is incapable of resolving the eyewall and eye (in this case, the diameter of the eye is effectively three grid points). While the initial vertical motion structure is not fully adequate, the upward motions obtained from the forecast on the 12-km grid very rapidly shift away from the center to form a more realistic eyewall (not shown). Thus, as will be shown in the next section, inadequacies in the initial vertical motions are not necessarily detrimental to the forecast.

2) FORECAST IMPACTS

Figure 7 shows the simulated tracks compared to the observed track of Hurricane Georges. All of the simulations produce tracks that are to the right of the observed motion. The two cases for which bogus SLP fields are assimilated (Expts. 1 and 3) show improved
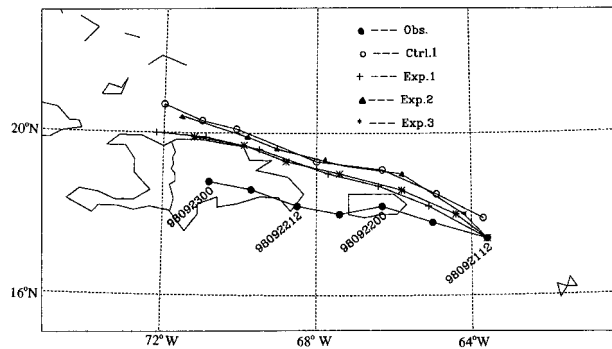
FIG. 7. Forecasts of hurricane track for the control run and Expts. 1–3 compared to the observed track. Center locations along the tracks are indicated every 6 h.

FIG. 8. Time series (at 6-h intervals) of (a) minimum SLP (hPa) and (b) maximum winds (m s^{-1}) at the lowest model level ($\sigma = 0.995$, approximately 50 m).

skill over the control simulation and the case involving assimilated winds only (Expt. 2). Experiments 1 and 3 provide a nearly 30% improvement in the track error but still lack a critical aspect of Georges's development: its direct interaction with the orography of Puerto Rico and the Dominican Republic.

Figure 8 compares the temporal variations of the minimum SLP (or hurricane central pressure, Fig. 8a) and maximum winds at the lowest model level with observations (Fig. 8b). The results suggest significant improvement in both the pressure and wind forecasts when bogus vortices are introduced into the initial conditions. However, there are marked differences between the experiments. In Expt. 1, in which only bogus SLP information was used, a dramatic spindown of the storm occurs within the first 6 h of the forecast, after which the case shows only marginal improvement over the control simulation. In Expt. 2, in which only bogus winds were used, the maximum wind forecast is reasonable, but the minimum SLP time series suggests an inadequate adjustment of the initial pressure field and a subsequent minimum pressure forecast that is usually higher than observed. However, the initial vortex generated by Expt. 2 results in a smooth start of the forecast and leads to a better intensity forecast than Expt. 1. These results are markedly different from Zou and Xiao (2000) and Xiao et al. (2000) and, as discussed in section 5, possibly arise from differences in vortex size and in the assumed wind and pressure profiles. Experiment 3, which uses both bogus SLP and wind information, provides the best forecast. The minimum central pressure and maximum winds are generally within 5–10 hPa and 5 m s^{-1}, respectively, of the observed values. In particular, note that the pressure rises and falls are comparable in behavior to the observed tendencies. While the observed movement of Georges over the island led to rapid weakening of the storm after 24 h, the more northward movement of the storm in Expt. 3 leads to less weakening.

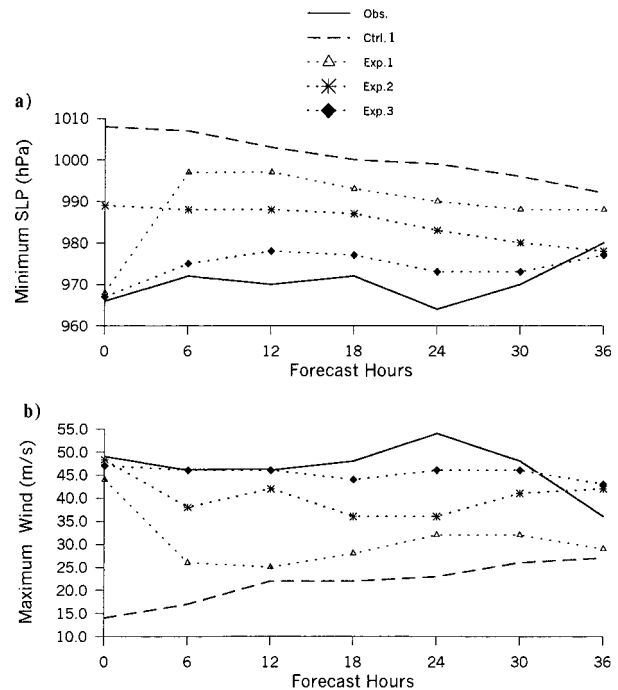The improvement of the forecast obtained by using bogus SLP and wind information is further demonstrated in Fig. 9, which shows forecasted 6-h precipitation accumulation for the control case and Expt. 3. In the control simulation (Fig. 9a), the vortex is weak and light precipitation covers a broad area to the north and east of the center. In Expt. 3 (Fig. 9b), intense precipitation occurs on the eastern side of the vortex with much lighter precipitation on the western side. Outer convective bands are seen well to the east of the center. Figure 9c shows the distribution of radar reflectivity from the lower-fuselage radar of the National Oceanic and Atmospheric Administration (NOAA) WP-3D reconnaissance aircraft at 1742 UTC 21 September, approximately 18 min prior to the time of Fig. 9b. The radar data indicate a qualitatively similar distribution of precipitation, with maximum rainfall on the eastern side of the storm center. The results show that the assimilation of the bogus pressure and wind fields leads not only to adjustments to those particular fields in the initial conditions, but also to significant adjustments to other fields such as moisture. Furthermore, despite the assimilation of axisymmetric distributions of pressure and wind, realistic asymmetries are produced for this case by the 4DVAR system.

d. Resolving inner-core structure

In the previous experiments, the bogus vortex was specified according to the observed size of the hurricane with an RMW comparable to the model grid spacing. Unrealistic upward vertical motion in the center of the hurricane was attributed to inadequate horizontal grid
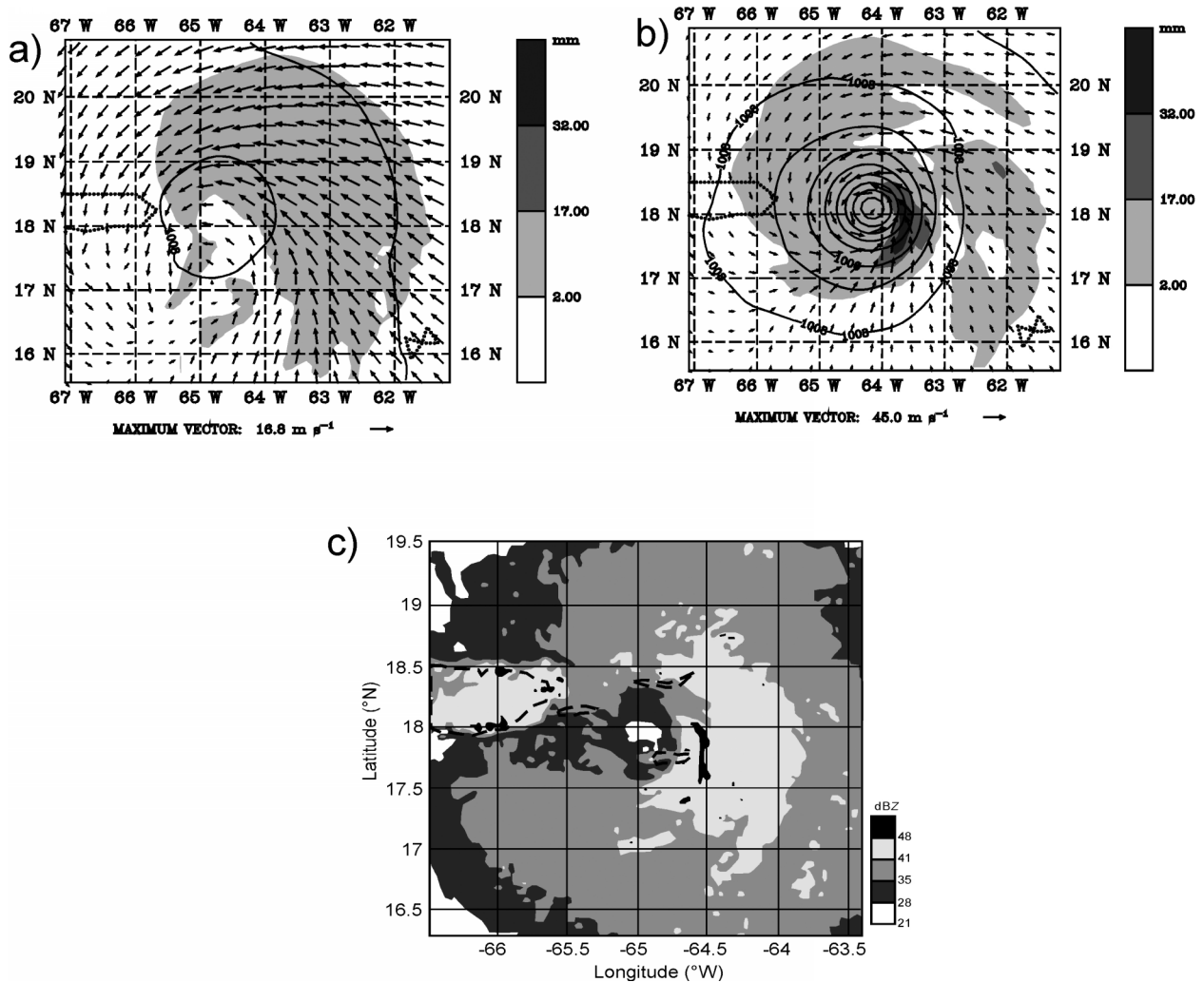
FIG. 9. Accumulated rainfall (shaded contours), SLP (solid line, contour interval 4 hPa), and wind vectors at lowest σ level at 6 h into the forecast valid at 1800 UTC 21 Sep for (a) the control simulation and (b) Expt. 3. (c) Radar reflectivity pattern from the lower fuselage of the NOAA P-3 reconnaissance aircraft valid at 1754 UTC 21 Sep (courtesy of NOAA's Hurricane Research Division). The dashed lines indicate orography including Puerto Rico.

resolution. This section explores the sensitivity of the assimilation and forecast to a bogus vortex of sufficient size such that it is resolved better by the 36-km grid spacing. Two experiments are performed:

- Expt. 4: Same as Expt. 1, except for an RMW of 120 km, instead of 40 km, and
- Expt. 5: Same as Expt. 3, except for an RMW of 120 km.

To illustrate the changes caused by the increased size of the vortex, Fig. 10 compares cross sections of wind speed through the center of the storm for Expts. 3 and 5. In Expt. 3 (Fig. 10a), the RMW is small and the model is unable to resolve the weak horizontal motions that should be present in the eye. In contrast, in Expt. 5 (Fig. 10b), the vortex is sufficiently large that the wind speed minimum in the eye is resolved.

Comparison of the vertical motions in Expt. 4 (Fig. 11a) with Expt. 1 (Fig. 4c) shows that even with the larger vortex, assimilation of only SLP information leads to strong upward motion near the center. In contrast, Fig. 11b shows that assimilation of both pressure and wind information associated with the larger vortex results in weaker vertical motion. In Expt. 3 (Fig. 6c), the upward motion was strongest near the center, but in Expt. 5 (Fig. 11b), the strongest upward motion is located to the east of the center with a suggestion of weak upward motion to the west and weak downward motion near the center below 350 hPa. Thus, *when the vortex is sufficiently large for it to be resolved on the horizontal grid, but not so large as to be unrealistic, improved vertical motion patterns are obtained.*

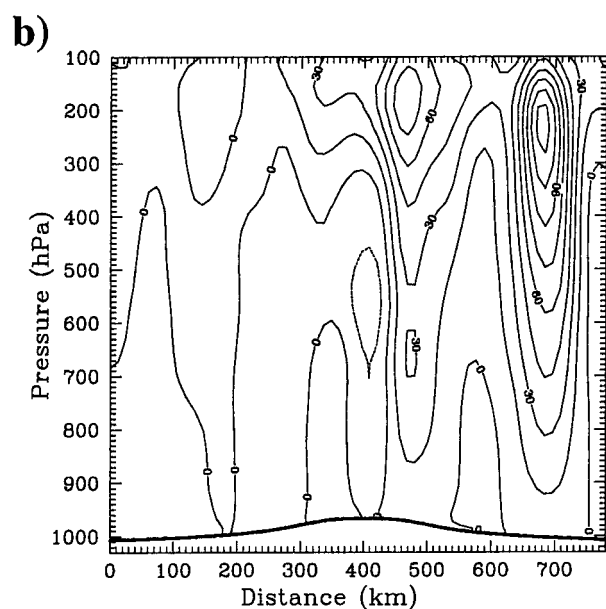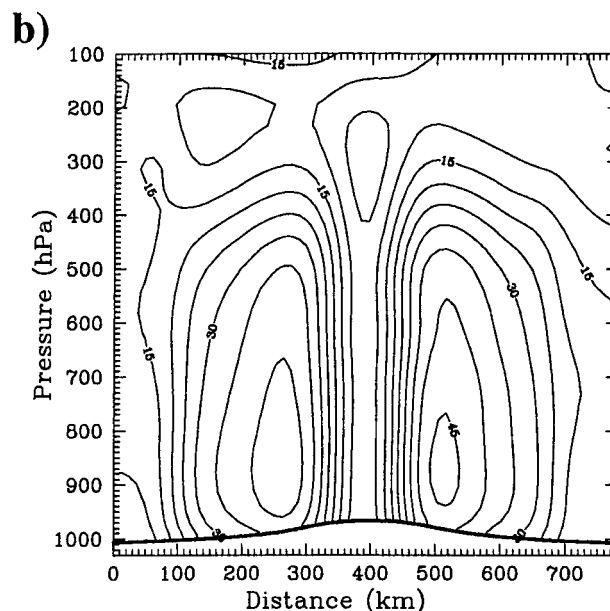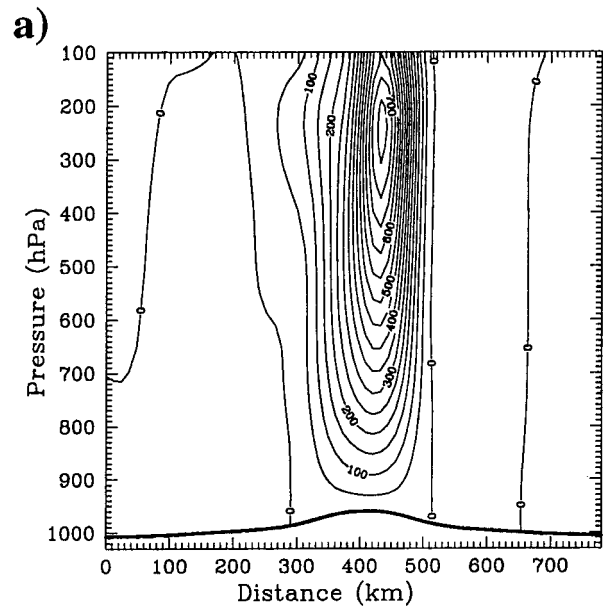The impact of vortex size on forecasts of track and intensity are shown in Figs. 12 and 13. The simulated
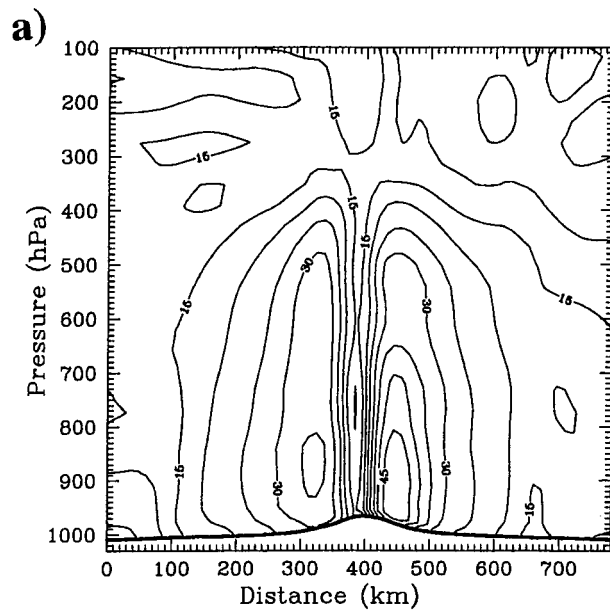
a)

b)

FIG. 10. East–west cross sections of wind speed through the center of vortex (17.4°N, 63.6°W) at the end of the assimilation window (30 min) for (a) Expt. 3 and (b) Expt. 5. The contour interval is 5 m s⁻¹.

a)

b)

FIG. 11. East–west cross sections of vertical velocity through the center of vortex (17.4°N, 63.6°W) at the end of the assimilation window (30 min) for (a) Expt. 4 and (b) Expt. 5. The contour interval is 50 cm s⁻¹ for (a) and 15 cm s⁻¹ for (b).

intensity in Expt. 4 (Fig. 13) is slightly better than in Expt. 1, but similar to Expt. 1, the initial vortex spins down very quickly at the beginning of the forecast integration (Fig. 13). The results for Expt. 5 show that both the track and intensity forecasts are improved tremendously. In particular, about 70% of the track error is reduced (Fig. 12) and the intensity forecast catches most features of the observed intensity changes (Fig.

13). The two landfalls of Hurricane Georges during this period are well predicted. The temporal variations of central SLP agree well with the observations (Fig. 13a) except for showing less of a rise in the final 12 h. This error may be due to the lack of high-resolution terrain information in the model. The forecast impacts suggest that using a vortex that is larger than observed may not be detrimental to the simulation, but in fact can provide
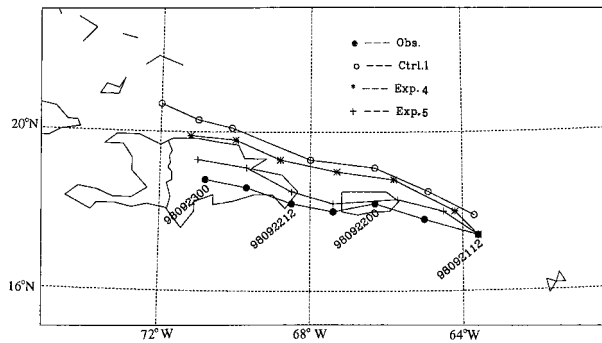
FIG. 12. Forecasts of hurricane track for the control run and Expts. 4 and 5 compared to the observed track. Center locations along the tracks are indicated every 6 h.

improved results as the vortex is resolved better on the model horizontal grid.

4. Hurricane Bonnie (1998)

The simulation of Hurricane Georges described in the previous section suggests a significant difference from the results of Xiao et al. (2000). Assimilation of SLP information alone failed to produce an adequate vortex and provided only marginal improvement of the forecast, while assimilation of wind information alone resulted in a much larger impact than in the case examined by Xiao et al. (2000). Since there may be some case-to-case variability in the model response to the bogus information, the bogusing techniques are applied to an additional case, that of Hurricane Bonnie (1998) just prior to its rapid intensification. Bonnie became a hurricane around 0000 UTC 22 August 1998. By 0600 UTC, reconnaissance aircraft detected a well-defined eyewall and flight-level winds up to 39 m s^{-1}. Over the next two days, Bonnie moved northwestward (Fig. 14) and developed maximum winds of 51 m s^{-1} and a minimum pressure of 954 hPa.

Similar to section 3, three experiments are performed for Hurricane Bonnie: the configurations of Expts. 6, 7, and 8 are similar to Expts. 1, 2, and 3 (see Table 1), respectively, except that all vortices are assigned an RMW of 120 km. The model includes an outer domain with 97 × 91 grid points and a 36-km grid spacing (domain C in Fig. 14) and a movable, nested domain with 145 × 127 grid points and 12-km grid spacing (domain D in Fig. 14). The model is integrated with ECMWF-derived analyses at 0000 UTC 22 August 1998. Assimilation of the bogus vortex is performed only for the 36-km domain, while initial conditions for the 12-km grid are interpolated from the coarser domain. The parameters defining the bogus vortex are as follows: p_c = 991 hPa at the hurricane center (21.1°N, 67.3°W), p_n = 1012 hPa, $\mathbf{V}_m$ = 33.5 m s^{-1}, and R_m = 120 km. The bogus information extends out to a radius of 300 km. Assimilation of the bogus vortex information is stopped after 30 iterations for all experiments.
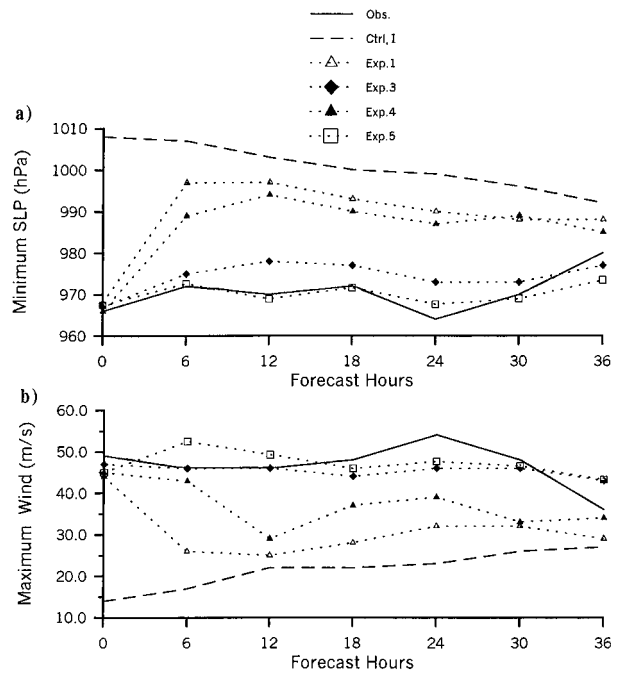

FIG. 13. Time series (at 6-h intervals) of (a) minimum SLP (hPa) and (b) maximum winds (m s^{-1}) at the lowest model level (σ = 0.995, approximately 50 m). Experiments 1 and 4 involve assimilation of SLP data only, while Expts. 3 and 5 involve assimilation of both pressure and winds.

Figure 15 shows the vector wind differences between the experiments (Expts. 6, 7, and 8) and the CTRL analysis as well as the divergence field at 850 hPa. The structural features in Fig. 15 are consistent with the features in Fig. 3. In the SLP only case (Expt. 6, Fig. 15a), the primary response of the wind field is in the divergent component with strong convergence in the center of the storm. When the winds alone are assimilated (Expt. 7, Fig. 15b), the response is primarily in the rotational component. The combination of wind and SLP information produces the best results, with strong convergence on the northern side of the vortex. The convergence is displaced from the center in the form of an eyewall rather than at the center (as in Fig. 15c or Fig. 3c) since the 120-km radius allows for better resolution of the eyewall and eye.

Four forecasting experiments are conducted, one without (Ctrl. 2) and the other three with the bogus vortices. Figure 16 shows the simulated tracks compared to the observed track of Bonnie. Without the bogus vortex, the control experiment shows significant errors in the initial position of the storm and a much too rapid movement to the northwest. Assimilation of the bogus information corrects the initial position error and reduces the subsequent track error, even capturing some of the slowing down of the storm late in the forecast period. In this case, assimilation of the wind information only (Expt. 7) produces a slightly a better track forecast than assimilation the SLP information only (Expt. 6).
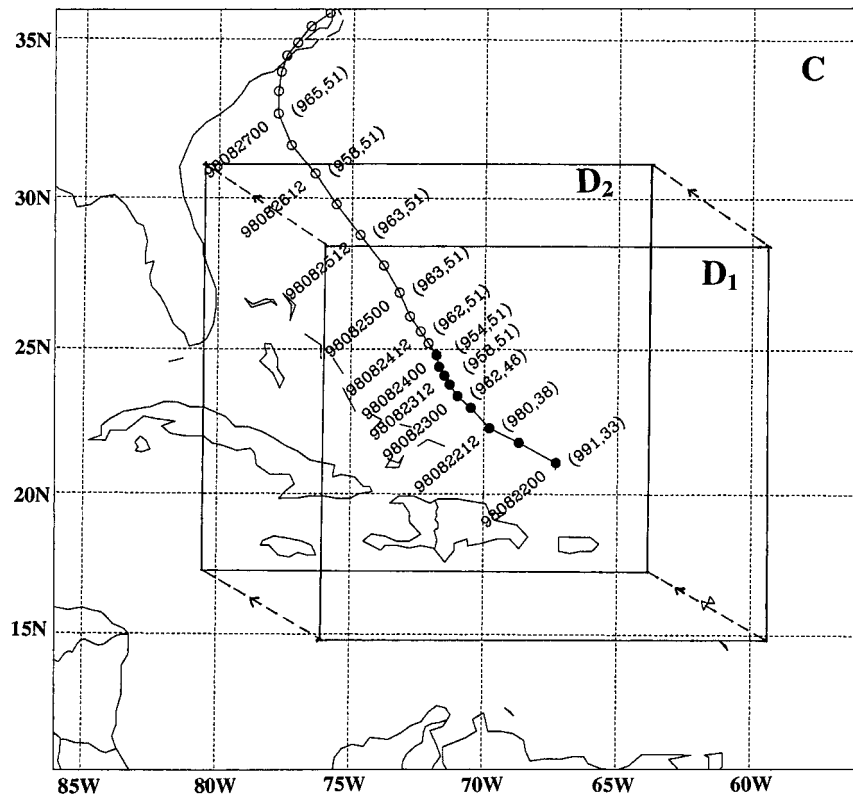
FIG. 14. Location of the model domains for the simulation of Hurricane Bonnie (1998). Domain C is the 36-km grid and domain D is the nested 12-km grid used in the forecast. Domain D is moved during the simulation from D1 to D2 at 18 h. Estimates of the center location at 6-h intervals are marked by circles. The minimum SLP (hPa) and maximum surface wind (m s^{-1}) are shown inside the brackets. The period included in the simulation is marked by the bold segment of the track.

Figure 17 shows the temporal variations of the minimum SLP (Fig. 17a) and maximum wind at the lowest model level (Fig. 17b). Clearly, with assimilation of the bogus vortices, the simulations are better able to reproduce the reduction of the central pressure and the increase in surface wind speed. However, different impacts are found among the three experiments. Assimilation of both SLP and wind data (Expt. 8) produces the best results with the forecasted pressure and wind very close to observations. With assimilation of bogus wind data only (Expt. 7), the SLP field is adjusted significantly after data assimilation, only about 2 hPa higher than observed, and results in a significant improvement of the intensity forecast. In contrast, when assimilating SLP information only (Expt. 6), the SLP of the generated initial vortex matches the observation very well, but the adjusted wind speed is inadequate compared with the observed value and the subsequent forecast skill is worse than Expts. 7 and 8.

5. Discussion

The simulation results for Hurricanes Georges and Bonnie presented in this study confirm the results of

Xiao et al. (2000, hereafter XZW) that assimilating both bogus SLP and wind information together provides the greatest benefit for forecasts, but they also highlight two key differences.

- Zou and Xiao (2000, hereafter ZX) and XZW suggested that assimilation of bogus SLP information alone was capable of producing a realistic vortex structure and intensity. The results of this study indicate that assimilation of SLP information alone results in a wind response that is dominated by the divergent component of the wind and yields a poorly defined vortex and smaller forecast improvement compared to other experiments.

- XZW found that assimilation of bogus wind data alone was insufficient for obtaining a realistic initial intensity (in terms of the SLP minimum), forecast of intensity change, and warm core structure within the eye. In this study, the assimilation of wind data alone generally provided a more realistic initial vortex structure, including a modest warm core. For Hurricane Georges, the initial SLP adjustment was significant (~20 hPa) but was insufficient to match observations, while for Hurricane Bonnie the initial SLP was very
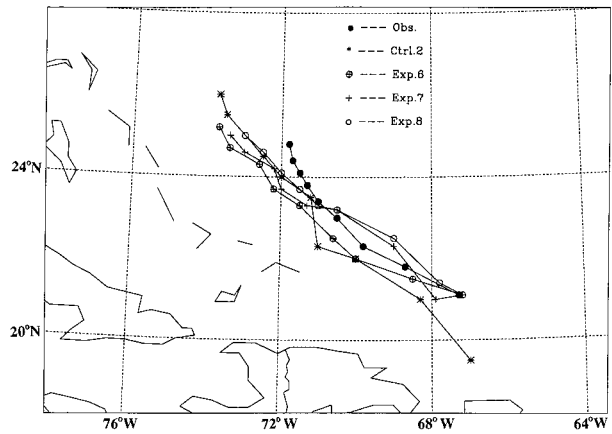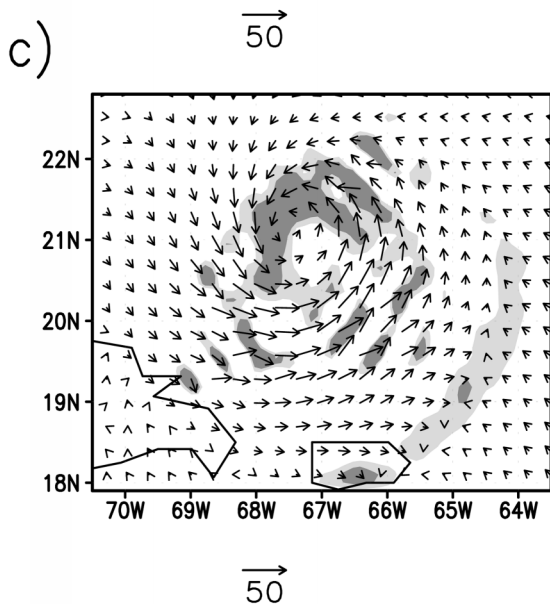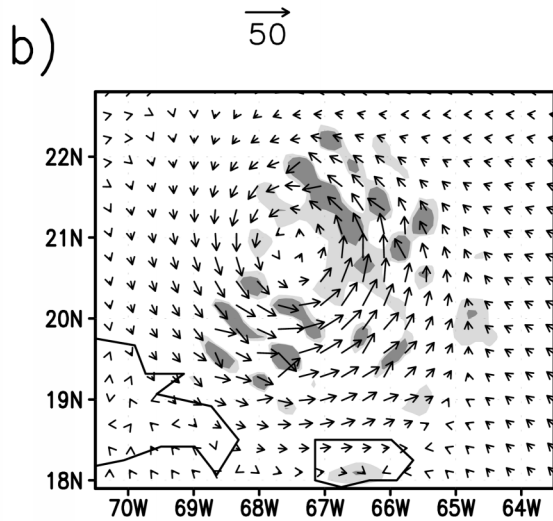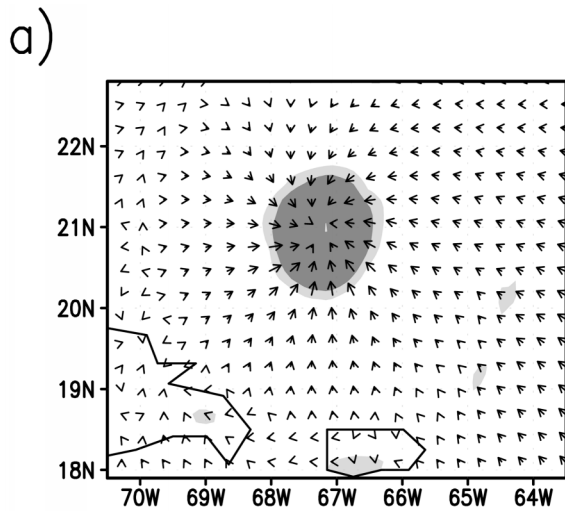
a)

b)

c)

FIG. 16. Forecasts of hurricane track for the control run and Expts. 6, 7, and 8 compared to the observed track. Center locations along the tracks are indicated every 6 h.

close to both the observed value and that obtained from the SLP-only case. In both cases, the forecasts from the wind-only cases after 6 h were superior to the cases in which only SLP information was assimilated.

These key differences can be reconciled to some extent. First, regarding the dominance of the divergent wind component in the model response to assimilation of the bogus SLP information, examination of Figs. 5 and 6 of ZX clearly implies a similar dominance of the divergent wind in their simulation of Hurricane Felix (1995). A simple explanation for this divergent wind response is that the assimilation of SLP information produces an initially strong isollobaric wind response and, because of the short 30-min assimilation window, Coriolis forces have insufficient time to transition the flow into gradient wind balance.

The different findings related to the improvement of the intensity forecasts associated with assimilation of bogus SLP information alone is likely driven primarily by vortex size and, to some extent, case-to-case variability. In their simulation of Hurricane Fran (1996), XZW examined the effect of vortex size by performing simulations with vortex radii at 80 km and ranging from 100 to 260 km at 40-km intervals. In these experiments, in which both bogus SLP and wind information were assimilated, the storm intensity increased as the radius was increased from 80 to 100 and 140 km and then continually decreased as the radius was gradually increased to 260 km. These results, combined with the simulations of Hurricane Georges described in section 3d, suggest that an optimal radius may exist that depends

←

FIG. 15. Same as Fig. 3, except (a) for Expt. 6, (b) for Expt. 7, and (c) for Expt. 8, and the shading scales, with light shading indicating values less than -10^{-4} s^{-1} and dark shading indicating values less than -2×10^{-4} s^{-1}.
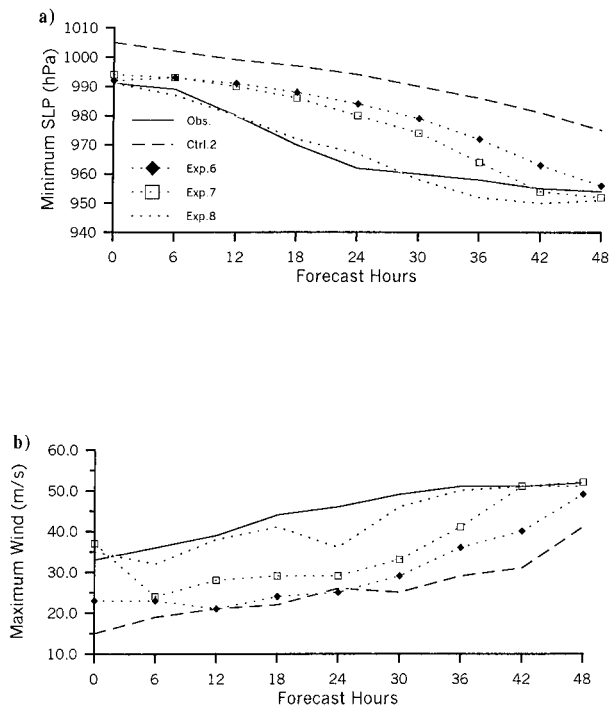
FIG. 17. Time series (at 6-h intervals) of (a) minimum SLP (hPa) and (b) maximum winds (m s^{-1}) at the lowest model level ($\sigma = 0.995$, approximately 50 m) for control simulation and Expts. 6, 7, and 8 compared to observations.

on the model grid spacing below which the vortex is insufficiently resolved and above which the size is unrealistically large, leading to degradation of the forecasts. The simulations of Hurricane Georges show that increasing the radius from 40 to 120 km increased the simulated intensity, consistent with the results of XZW. However, forecasts from both Georges and Bonnie using a radius of 120 km and assimilated SLP information resulted in simulated intensities that were significantly less than observed. Case-to-case variability must be considered as a factor given the range of possible errors in the large-scale environmental conditions between different cases as well as the selection and performance of different model physics options (e.g., cumulus parameterizations).

The different impacts of assimilated winds (without SLP information) are also attributed to vortex size, and to some extent, to the assumed pressure and wind profiles. XZW used profiles for which vortex size was specified by the radius of maximum SLP gradient (R_G), which, according to the gradient wind relation [Eq. (2) of XZW], results in a radius of maximum winds that is larger than R_G. XZW used a radius of $R_G = 220$ km for their experiments with wind data only and SLP only, which yielded a radius of maximum winds greater than 300 km (see Fig. 13a of XZW). With this vortex size, they found that assimilation of wind data alone produced about a 2-hPa decrease in SLP compared to their control simulation without bogus data. For the two cases in this

study, however, bogus wind assimilation resulted in adjustments to SLP of about 50% of the initial SLP error (20 hPa) for Georges using a 40-km radius and 80% of the initial SLP error (12 hPa) for Bonnie using a 120-km radius. These results suggest that the bogus wind data impacts depend on the size of the specified vortex and may become small if the radius of the vortex become too large.

6. Conclusions

The effectiveness of four-dimensional variational assimilation techniques for creating bogus vortices in numerical simulations of hurricanes is examined using the PSU–NCAR nonhydrostatic model (MM5) and its adjoint system. The variational bogus vortex assimilation methodology is applied to simulations of Hurricanes Georges and Bonnie (1998) using different approaches: 1) assimilation of bogus SLP information only, 2) assimilation of bogus wind information only, and 3) assimilation of both bogus SLP and wind information. The bogus information is assimilated within a 30-min assimilation window in order to generate initial vortices that are consistent with the model resolution and physics.

Experiments in which both bogus SLP and wind information are assimilated clearly produce the most reasonable initial vortex structures and the best forecasts. When only SLP information is assimilated, the initial response of the horizontal wind field is dominated by the divergent component of the wind, leading to strong low-level convergence, upper-level divergence, and strong upward motion in the center of the storm. In both Hurricanes Georges and Bonnie, the least skillful forecasts are obtained when assimilating SLP only. Assimilation of the wind data only produces a wind response dominated by the rotational component of the wind. In the case of Hurricane Georges, the bogus winds lead to a 20-hPa decrease in central pressure and a realistic vortex. Although the intensity of the simulated storm is initially weaker than that of the SLP-only case, the subsequent forecast gradually leads to a more intense storm. For Hurricane Bonnie, assimilation of only wind information produces a 12-hPa decrease in central pressure and, again, a better intensity and track forecast than that obtained from assimilating SLP information only. These results differ with those of Xiao et al. (2000), who found only very minor impact in the case of Hurricane Fran (1996) when assimilating winds only. When both bogus wind and SLP information are assimilated together, the response of the wind field contains both strong rotational and divergent components and the simulations produce intensity forecasts in good agreement with observations.

Inclusion of both bogus wind and SLP information essentially provides the assimilation system with a gradient wind balance constraint since the bogus winds are derived from the SLP information by assuming gradient wind balance. The strongly divergent wind fields in the

SLP-only cases clearly suggest an unbalanced response to the SLP information and a necessity for some type of balance constraint. On the other hand, when only the bogus wind data are assimilated, a more balanced model response is obtained. The ability of the 4DVAR system to correct the initial intensity error and improve the forecast is sensitive to the size of the vortex, the results suggest that when specifying the size of the bogus vortex, careful consideration should be given not only to the observed size, but also to what size can be resolved on the horizontal grid while keeping the size within reasonable limits. The substantial impact of the bogus wind data suggests a large potential for improvement of model initial conditions and forecasts of hurricane track and intensity by using satellite remotely sensed winds such as those derived from scatterometers (e.g., the National Aeronautics and Space Administration's QuikScat satellite), particularly when pressure information is unavailable or highly uncertain.

References

Bender, M. A., R. J. Ross, R. E. Tuleya, and Y. Kurihara, 1993: Improvements in tropic cyclone track and intensity forecasts using the GFDL initialization system. *Mon. Wea. Rev.,* **121,** 2046–2061.

Blackadar, A. K., 1976: Modeling the nocturnal boundary layer. Preprints, *Third Symp. on Atmospheric Turbulence, Diffusion, and Air Quality,* Raleigh, NC, Amer. Meteor. Soc., 46–49.

——, 1979: High resolution models of the planetary boundary layer. *Advances in Environmental Science and Engineering,* Vol. 1, No. 1, J. Pfafflin and E. Ziegler, Eds., Gordon and Breach, 50–85.

Dudhia, J., 1993: A nonhydrostatic version of the Penn State–NCAR mesoscale model: Validation tests and simulation of an Atlantic cyclone and cold front. *Mon. Wea. Rev.,* **121,** 1493–1513.

Grell, G. A., J. Dudhia, and D. R. Stauffer, 1995: A description of the fifth-generation Penn State/NCAR mesoscale model (MM5). NCAR Technical Note, NCAR/TN-398+STR, 138 pp. [Available from NCAR Publications Office, P.O. Box 3000, Boulder, CO 80307-3000.]

Holland, G. 1980: An analytic model of the wind and pressure profile in hurricanes. *Mon. Wea. Rev.,* **108,** 1212–1218.

Iwasaki, T., H. Nakano, and M. Sugi, 1987: The performance of a typhoon track prediction model with cumulus parameterization. *J. Meteor. Soc. Japan,* **65,** 555–570.

Kuo, Y.-H., X. Zou, and Y. R. Guo, 1996: Variational assimilation of precipitable water using a nonhydrostatic mesoscale adjoint model. Part I: Moisture retrieval and sensitivity experiments. *Mon. Wea. Rev.,* **124,** 122–147.

Kurihara, Y., M. A. Bender, R. E. Tuleya, and R. J. Ross, 1990: Prediction experiments of Hurricane Gloria (1985) using a multiply nested movable mesh model. *Mon. Wea. Rev.,* **118,** 2185–2198.

——, ——, and R. J. Ross, 1993: An initialization scheme of hurricane models by vortex specification. *Mon. Wea. Rev.,* **121,** 2030–2045.

Leslie, L. M., and G. J. Holland, 1995: On the bogussing of tropical cyclones in numerical models: A comparison of vortex profiles. *Meteor. Atmos. Phys.,* **56,** 101–110.

Lord, S. J., 1991: A bogusing system for vortex circulations in the National Meteorological Center global forecast model. Preprints, *19th Conf. on Hurricane and Tropical Meteorology,* Miami, FL, Amer. Meteor. Soc., 328–330.

Manning, K. W., and P. L. Haagenson, 1992: Data ingest and objective analysis for the PSU/NCAR modeling system: Programs DATAGRID and RAWINS. NCAR Tech. Note (NCAR/TN-376+IA), 209 pp. [Available from NCAR Publications Office, P.O. Box 3000, Boulder, CO 80307-3000.]

Mathur, M. B., 1991: The National Meteorological Center's quasi-Lagrangian model for hurricane prediction. *Mon. Wea. Rev.,* **119,** 1419–1447.

Smolarkiewicz, P. K., and G. A. Grell, 1992: A class of monotone interpolation schemes. *J. Comput. Phys.,* **101,** 431–440.

Trinh, V. T., and T. N. Krishnamuti, 1992: Vortex initialization for Typhoon track prediction. *Meteor. Atmos. Phys.,* **47,** 117–126.

Xiao, Q., X. Zou, and B. Wang, 2000: Initialization and simulation of a landfalling hurricane using a variational bogus data assimilation scheme. *Mon. Wea. Rev.,* **128,** 2252–2269.

Zhang, D.-L., and R. A. Anthes, 1982: A high-resolution model of the planetary boundary layer—Sensitivity tests and comparisons with SESAME-79 data. *J. Appl. Meteor.,* **21,** 1594–1609.

Zou, X., and Q. Xiao, 2000: Studies on the initialization and simulation of a mature hurricane using a variational bogus data assimilation scheme. *J. Atmos. Sci.,* **57,** 836–860.

——, W. Huang, and Q. Xiao, 1998: A user's guide to the MM5 adjoint modeling system. NCAR TN-437+IA, MMM division, NCAR, 94 pp. [Available from NCAR Publications Office, P.O. Box 3000, Boulder, CO 80307-3000.]